Soft-x-ray lasing to the ground states in low-charged oxygen ions

B.N. Chichkov,* A. Egbert, H. Eichmann, C. Momma, S. Nolte,
and B. Wellegehausen
Institut für Quantenoptik, Universität Hannover, Welfengarten 1, D-30167 Hannover, Germany
(Received 16 December 1994)

Optimal schemes for the creation of a transient population inversion between the ground and excited states of an ion in a subpicosecond-pulse laser-produced plasma are discussed. First results on experimental investigations of possible amplification in the soft-x-ray spectral region on transitions to the ground states in O II, O III, C III, and N III ions are reported. Ions are produced due to optical field ionization of O_2, CO_2, and N_2 gases in an intense Ti:sapphire laser field. Amplification on the $2p3s(^3P)$-$2p^2(^3P)$ transition ($\lambda = 374.12$ Å) in O III ions and on the $2p^23s(^2P)$-$2p^3(^2D)$ transition ($\lambda = 616.56$ Å) in O II ions has been observed.

PACS number(s): 42.55.Vc, 52.50.Jm, 52.25.−b

I. INTRODUCTION

The recent availability and rapid progress of intense ultrashort-pulse laser systems has led to growing interest in the development of high-repetition-rate soft-x-ray lasers driven by short laser pulses. With the help of these intense laser pulses any kind of matter can be rapidly ionized on a time scale comparable to or shorter than the characteristic relaxation times of ion states. This can result in a transient population inversion between the ground and excited ion states and amplification of radiation in the soft-x-ray region.

One of the most popular soft-x-ray laser approaches is based on optical field (tunnel) ionization of atoms in an intense laser field [1, 2]. This ionization mechanism is very selective (due to the exponential dependence of the ionization rate on laser intensity and ionization potential) and allows one to strip all atoms to a necessary, definite ionization stage. In the case of a linearly polarized laser field, the free electrons can be left relatively cold, which allows one to create a transient population inversion between excited and ground ion states during the three-body recombination cascade. The transient gain is very sensitive to the residual amount of ions occupying the lower lasing level [2]. Up until now, theoretical studies of a possible x-ray lasing to the ground ion state were concentrated on H- and Li-like ions [1, 2]. Recent experimental results [3] have demonstrated evidence of amplification in H-like Li ions at 135 Å on the L_α transition. This evidence is not overwhelming and there are still some contradictions [3, 4]. In the case of a circular polarized laser field, the ionized electrons are hot and can provide efficient collisional excitation pumping. Demonstration of xuv lasing due to this mechanism at 418.1 Å in Xe IX ions has recently been reported [5].

In this paper, we try to identify more suitable routes and schemes for the creation of population inversion and soft-x-ray lasing to the ground state. Our simple theoretical analysis, presented in Sec. II of this paper, shows that conditions necessary for the soft-x-ray lasing to the ground electron configuration can be easier realized with more complex ions. A trivial argument for this conclusion follows immediately from the expression for the population inversion density $\Delta N = N_2 - N_1 g_2/g_1$, where g_1 and g_2 are the statistical weights for the lower and upper laser levels. It is clear that more favorable conditions for the population inversion will be obtained between levels with g_1/g_2 as large as possible ($g_1/g_2 \to \infty$). For the L_α transition in H-like ions $g_1/g_2 = 1/3$. In Sec. III, plasma parameters and inversion schemes for Be-, B-, C-, and N-like ions are discussed. In Sec. IV, experimental results obtained with O II, O III, C III, and N III ions for transitions with $g_1/g_2 \geq 1$ are presented.

II. ON THE GENERAL CONDITIONS REQUIRED FOR POPULATION INVERSION TO THE GROUND STATE

Ground-state lasers are nothing unusual. For example, the well-known 694-nm ruby laser—the first laser ever to be operated—is a ground-state laser. From the experience with ground-state optical lasers, it is known that they need higher pumping rates for their operation than lasers with the working transition between excited levels, and that they can be reasonably well modeled by a simple three-level scheme (see, for example, [6]). Therefore, to find an optimal way for the creation of an inversion between the ground and excited states of an ion we also consider an idealized three-level model (see Fig. 1).

Two neighbor ion stages connected by a pumping process (three-body recombination cascade) having the rate W_p [s^{-1}] are assumed. This pumping produces the required ion population directly in the upper laser state. It is also assumed that the radiation corresponding to the 2-1 transition (A_{21} is the probability of the spontaneous radiative decay) is still weak enough so that stimulated transitions can be neglected. The trivial rate equations

*Permanent address: P.N. Lebedev Physical Institute, Leninsky prospect 53, Moscow, Russia.

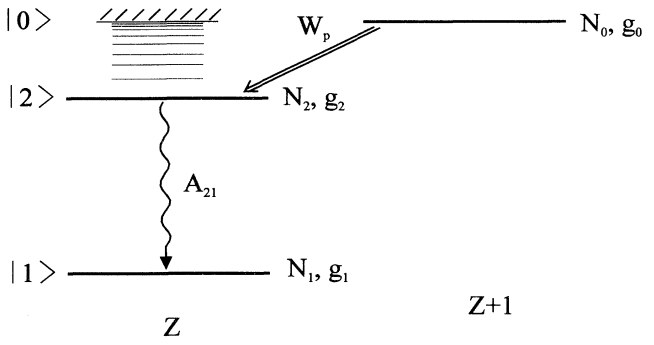

FIG. 1. Idealized three-level scheme for the ground-state soft-x-ray laser.

for the populations N_i of the various states are then

$$\frac{dN_0}{dt} = -N_0 W_p, \quad \frac{dN_2}{dt} = N_0 W_p - N_2 A_{21},$$
$$\frac{dN_1}{dt} = N_2 A_{21}, \tag{1}$$

where $N_0 + N_1 + N_2 = N$ is the constant total population, and for $t = 0$ the initial conditions are $N_0 = N - n$, $N_2 = 0$, $N_1 = n$, with n being the initial population of the ground state. Note that the probability of the stimulated transition in the active medium is equal to $A_{21}\nu d\Omega/4\pi$, where ν is the average number of photons per mode corresponding to the 2-1 transition and $d\Omega$ is the solid angular size of the active medium (usually $d\Omega/4\pi \sim 10^{-5}$–$10^{-3}$). Therefore, the isotropic spontaneous decay will still dominate the stimulated decay up to rather high values of ν.

The formal solution of the above rate equations with W_p depending on time is given by

$$N_0 = (N-n)\exp\left(-\int_0^t W_p(t')dt'\right),$$
$$N_2 = (N-n)\exp(-A_{21}t)\int_0^t W_p(t') \times \exp\left(-\int_0^{t'}[W_p(t'') - A_{21}]dt''\right)dt'. \tag{2}$$

N_1 is then found from the conservation of particles. The corresponding time evolution of the population inversion $\Delta N = N_2 - N_1 g_2/g_1$ is

$$\Delta N = \frac{g_2}{g_1}\left\{(N-n)\exp(-A_{21}t)\int_0^t [W_p(t')g_1/g_2 + A_{21}] \times \exp\left[-\int_0^{t'}[W_p(t'') - A_{21}]dt''\right]dt' + (N-n)\exp(-A_{21}t) - N\right\}. \tag{3}$$

For a general consideration we can assume that the pumping rate is constant during the rather short time interval when an inversion can occur. In this case,

$$\Delta N = \frac{g_2}{g_1}N(1-\beta)\left\{\frac{g_1/g_2+\gamma}{\gamma-1}\exp(-\tau/\gamma) - \frac{1+g_1/g_2}{\gamma-1}\exp(-\tau) - \frac{1}{1-\beta}\right\}, \tag{4}$$

where $\beta = n/N$, $\gamma = A_{21}/W_p$, and $\tau = A_{21}t$. Note, that for the special case, where $\gamma = 1$, Eq. (4) reduces to

$$\Delta N = \frac{g_2}{g_1}N(1-\beta)[\exp(-\tau) + (g_1/g_2+1)\tau\exp(-\tau) - (1-\beta)^{-1}]. \tag{5}$$

For small τ, the population inversion (4) is given by $\Delta N = N[-\beta g_2/g_1 + (1-\beta)\tau/\gamma]$. Initially, it is negative and its growth rate $(1-\beta)/\gamma$ is independent of the ratio g_1/g_2.

In Figs. 2(a)–2(c) the time dependence of the relative population inversion $\Delta N/N$ is shown for various

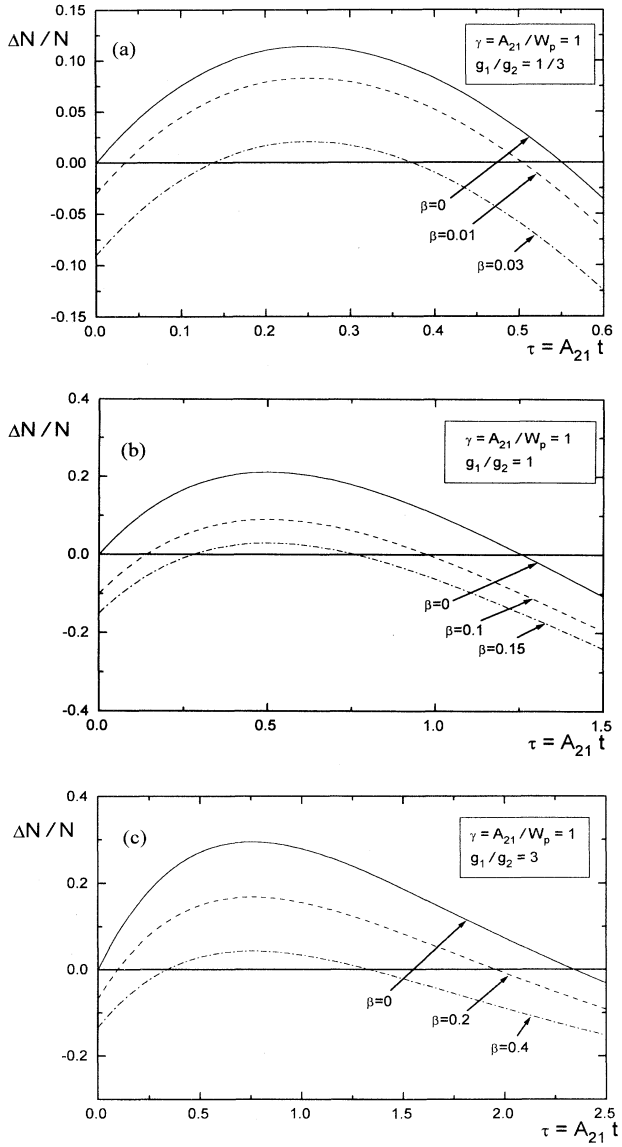

FIG. 2. Time dependence (a)–(c) of the relative population inversion for different ratios of g_1/g_2 and initial populations of the ground state, $\beta = N_1/N$.

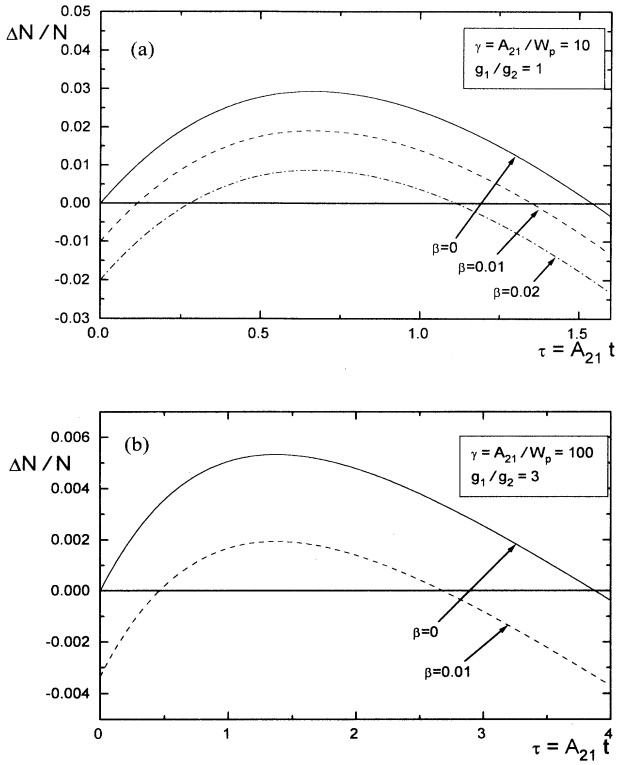

FIG. 3. Same as Fig. 2 for lower pumping rates.

g_1/g_2 ratios and initial populations of the ground level, $\beta = N_1/N$. Calculations are performed for a high pumping rate, $W_p = A_{21}$ or $\gamma = 1$. It is trivial that the positive inversion always exists if the initial population of the ground state is exactly zero, ($\beta = 0$). The corresponding curves, with $\beta = 0$, are shown in Figs. 2(a)–2(c) to demonstrate the limiting values of a possible population inversion and its duration. The time behavior shown in Fig. 2(a) models the case of the L_α transition in H-like ions with $g_1/g_2 = 1/3$. As can be seen, for the creation of a population inversion on the L_α transition, the initial population of the ground level should be very low, $\beta \sim 10^{-2}$. For the lower pumping rate, $W_p \sim A_{21}/10$, the allowed value of the initial population reduces to $\beta \sim 10^{-3}$. This conclusion coincides with the predictions of detailed calculations [2]. The creation of such low initial populations of the ground level and, at the same time, realization of high pumping rates is a very difficult experimental problem.

In Figs. 2(b) and 2(c) it is shown that more favorable conditions exist for transitions with larger g_1/g_2 ratios. In this case, for a high pumping rate, $W_p = A_{21}$, the allowed initial populations of the ground levels can be much higher. For transitions with $g_1/g_2 = 3$, for example, the inversion can be created even when $\beta = 0.4$. An additional advantage is the possibility of a considerable reduction of the pumping rate, as it is shown in Fig. 3(a) for $W_p = A_{21}/10$ and Fig. 3(b) for $W_p = A_{21}/100$. It is essential that for these much lower pumping rates the allowed initial population of the ground state is the same as in Fig. 2(a) for the L_α transition.

The time of the maximum inversion, $\tau = \tau_{\max}$, can be found from the condition $d(\Delta N)/d\tau = 0$,

$$\tau_{\max} = \frac{\gamma}{\gamma - 1} \ln \frac{(1 + g_1/g_2)\gamma}{g_1/g_2 + \gamma}, \tag{6}$$

where for $\gamma = 1$ $\tau_{\max} = g_1/(g_1 + g_2)$. Note that $\tau_{\max}$ is independent of β. When $\beta \neq 0$ the population inversion at the moment $\tau = \tau_{\max}$ can still be negative. It crosses the zero level $\Delta N(\tau_{\max}) = 0$ when $\beta = \beta_{\rm cr} = 1 - (1 + g_1/g_2)^{-1} \exp(\tau_{\max})$. This function is shown in Fig. 4 for different ratios of g_1/g_2. A positive inversion exists for $\beta < \beta_{\rm cr}$. It can be clearly seen that the region of the parameter space available for the creation of inversion becomes larger with the growth of the ratio g_1/g_2.

In the next section we present examples of the more favorable soft-x-ray laser schemes and discuss plasma parameters that can be created due to optical field ionization.

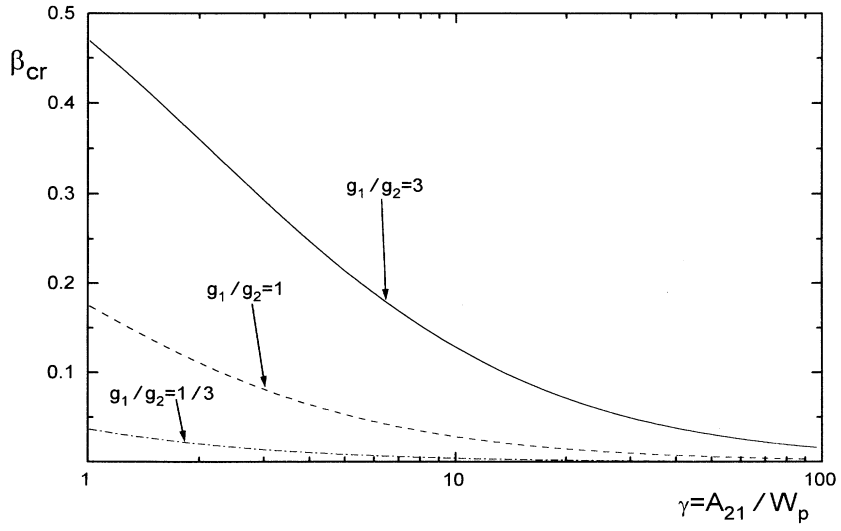

FIG. 4. Critical values for the allowed initial populations of the ground state.

III. PLASMA PARAMETERS AND INVERSION SCHEMES

Atoms and molecules in an intense short-pulse laser field undergo rapid ionization. Each new ion state is created when the laser intensity reaches the level of the so-called appearance intensity I_a, which is well predicted by a simple overbarrier model [7] $I_a = I_{at}E_i^4/256\mathcal{R}^4Z^2 = 4.0\times10^9 E_i^4/Z^2$ W/cm^2, where $I_{at} = 3.5\times10^{16}$ W/cm^2 is the atomic intensity, $\mathcal{R} = 13.6$ eV, E_i is the ionization energy of the atom (ion) in eV and Z is the charge of the produced ion. The ionization mechanism is usually characterized by the Keldysh parameter $\gamma = (E_i/2U_p)^{1/2}$ [8], where $U_p = e^2E^2/4m\omega^2$ is the average energy of electron oscillations (ponderomotive potential) in a linearly polarized laser field with the amplitude E. Introducing the appearance intensity in the above expressions, we obtain $U_p = E_i^4/128\mathcal{R}Z^2\omega^2$ for the ponderomotive potential and $\gamma = 8Z\omega(\mathcal{R}/E_i^3)^{1/2}$ for the Keldysh parameter, where ω and E_i are in eV. Ionization occurs in the tunneling regime when $\gamma < 1$ or $E_i > 4\mathcal{R}^{1/3}(Z\omega)^{2/3}$. In our experiments (see Sec. IV) the laser frequency is $\omega = 1.6$ eV and the condition for tunnel ionization of atoms and molecules ($Z = 1$) can be written as $E_i > 13$ eV. This condition is approximately fulfilled in our experiments with O_2, CO_2, and N_2 gases.

In a series of papers [9], it was shown that in the tunneling regime the simple molecules are ionized as if they were structureless atoms with an ionization potential equivalent to that of the molecular ground state. In this case, the electron distribution function after the tunnel ionization in a linearly polarized laser field can be written in the form [10] (here the asymptotically correct value for the normalization constant is introduced)

$$F(\mathcal{E})d\mathcal{E} = \sqrt{\frac{b}{2\pi}}\left(1-\frac{\mathcal{E}}{2U_p}\right)^{-1}\left(\frac{\mathcal{E}}{2U_P}\right)^{-1/2} \times \exp\left[b-b\left(1-\frac{\mathcal{E}}{2U_p}\right)^{-1/2}\right]\frac{d\mathcal{E}}{2U_p}, \quad (7)$$

$$b = \frac{2}{3}\left(\frac{E_i}{\mathcal{R}}\right)^{3/2}\frac{E_{at}}{E} \gg 1,$$

where $\mathcal{E}$ is the electron energy, $E_{at} = 5.1\times10^9$ V/cm is the atomic unit of field strength, and E is the amplitude of the laser field. This electron distribution results from the quasistatic model for tunnel ionization. It is easy to show that in the most important case, when $\mathcal{E} \ll 2U_p$, the distribution (7) transforms into the one-dimensional Maxwellian distribution with respect to energy $F(\mathcal{E}) = (\pi T\mathcal{E})^{-1/2}\exp(-\mathcal{E}/T)$ or momentum $f(p) = (2\pi T)^{-1/2}\exp(-p^2/2T)$, where $T = 3/2\times E^3/(2E_i)^{3/2}\omega^2$ is the electron temperature in atomic units.

In a more consistent approach [11] the probabilities of tunnel ionization into free-electron states with a definite momentum were derived. After renormalization of these probabilities, one can obtain the following electron distribution function $f(\mathbf{p})d^3\mathbf{p} = f(p_\parallel)f(\mathbf{p}_\perp)dp_\parallel d^2\mathbf{p}_\perp$, where (atomic units are used):

$$f(p_\parallel) = (2\pi T_\parallel)^{-1/2}\exp\left(-\frac{p_\parallel^2}{2T_\parallel}\right),$$
$$f(\mathbf{p}_\perp) = (2\pi T_\perp)^{-1}\exp\left(-\frac{\mathbf{p}_\perp^2}{2T_\perp}\right), \quad (8)$$
$$T_\parallel = \frac{3}{2}\frac{E^3}{(2E_i)^{3/2}\omega^2}, \qquad T_\perp = \frac{E}{2(2E_i)^{1/2}}.$$

A simple derivation of this and other electron distributions and comparison with available experimental data will be published elsewhere [12]. The electron distribution function (8) is strongly anisotropic in directions ($\parallel$) and ($\perp$) to the laser field, since usually $T_\parallel \gg T_\perp$. Note that the distribution with respect to $p_\parallel$ coincides with the distribution obtained above from (7).

The distribution function with respect to electron energy corresponding to the two-temperature Maxwellian distribution (8) can be written as $F(\mathcal{E})d\mathcal{E} = F_M(\mathcal{E})\,\Phi_a d\mathcal{E}$,

$$F_M = 2\pi^{-1/2}T^{-3/2}\sqrt{\mathcal{E}}\exp(-\mathcal{E}/T),$$
$$\Phi_a = \frac{T^{3/2}}{T_\perp T_\parallel^{1/2}}\int_0^1 \exp\left[\frac{\mathcal{E}}{T}(1/T_\perp - 1/T_\parallel)(Tx^2 - T_\parallel/3)\right]dx, \quad (9)$$

with $T = (T_\parallel + 2T_\perp)/3$, where F_M is the Maxwellian distribution function and Φ_a takes into account the temperature anisotropy. In Fig. 5, this distribution function is shown for constant temperature T and several ratios of $T_\parallel/T_\perp$. As can be seen, the density of cold electrons increases with the growth of anisotropy.

Tunnel-ionized plasmas and relaxation of strong temperature anisotropy have been recently studied experimentally and theoretically using particle simulations [13]. It has been shown that a crucial role in the temperature isotropization is played by the Weibel instability. Expressions for the temperature isotropization time scale due to this mechanism can be found in [13]. A more

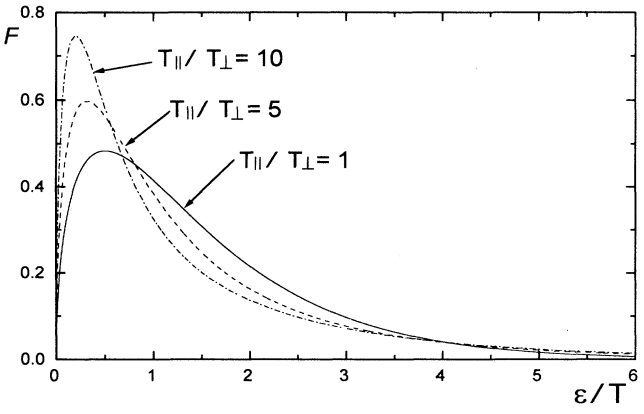

FIG. 5. Two-temperature Maxwellian distribution function (9).

detailed discussion of relaxation processes is beyond the scope of this paper and will be published elsewhere [12].

After relaxation of the strong temperature anisotropy ($T_{\|} \ll T_{\perp}$) the electron distribution becomes Maxwellian with the temperature

$$T \simeq T_{\|}/3 = 4\mathcal{R}^{9/2}(E/E_{\rm at})^3/E_i^{3/2}\omega^2.$$

To estimate this temperature we again use the ion appearance intensity. This gives

$$T = 2^{-10}\frac{E_i^{9/2}}{Z^3\omega^2\mathcal{R}^{3/2}}, \tag{10}$$

where ω is in units of energy. This temperature rapidly increases with the ion charge. For example for H-like ions it is given by $T = 2^{-10}Z^6\mathcal{R}^3/\omega^2$. Therefore, in order to keep the electrons cold, it is advantageous to work with relatively low ion states. The expressions derived above provide an estimate of the plasma parameters created after tunnel ionization.

Now we turn to the discussion of ion candidates that are more favorable for the creation of an inversion to the ground states. We consider low-charged ions with a partially filled L shell. In Figs. 6(a) and 6(b) the energy levels, wavelengths (in Å), and radiative decay probabilities (in s^{-1}) for transitions in O III and O II ions are shown. If the laser intensity is high enough to ionize most of the oxygen atoms (molecules) to the O IV stage, and if the free electrons are left cold, then due to the three-body recombination cascade an inversion can be created on the $2p3s(^3P)$-$2p^2(^3P)$ transition ($g_1/g_2 = 1$) in O III ions. The laser intensity I_l which is necessary for ionization of O III ions ($E_i = 54.936$ eV) is $I_l > I_a = 4.0 \times 10^{15}$ W/cm^2. The ionization of O IV ions ($E_i = 77.414$ eV) begins when $I_l = I_a = 9 \times 10^{15}$ W/cm^2. Thus, for the realization of inversion in O III ions the laser intensity should be $I_l \sim 10^{16}$ W/cm^2.

Three different types of Maxwellian distributions will be created after the tunnel ionization of oxygen atoms in the short pulse laser field ($\omega = 1.6$ eV), with the effective temperatures $T_i = 7.6 \times 10^{-6}E_i^{9/2}/Z^3$ eV found from (10), where $T_1 = 0.96$, $T_2 = 8.5$, and $T_3 = 18.9$ eV. These distributions are created due to successive ionization of oxygen atoms, single charged ions, etc. Note

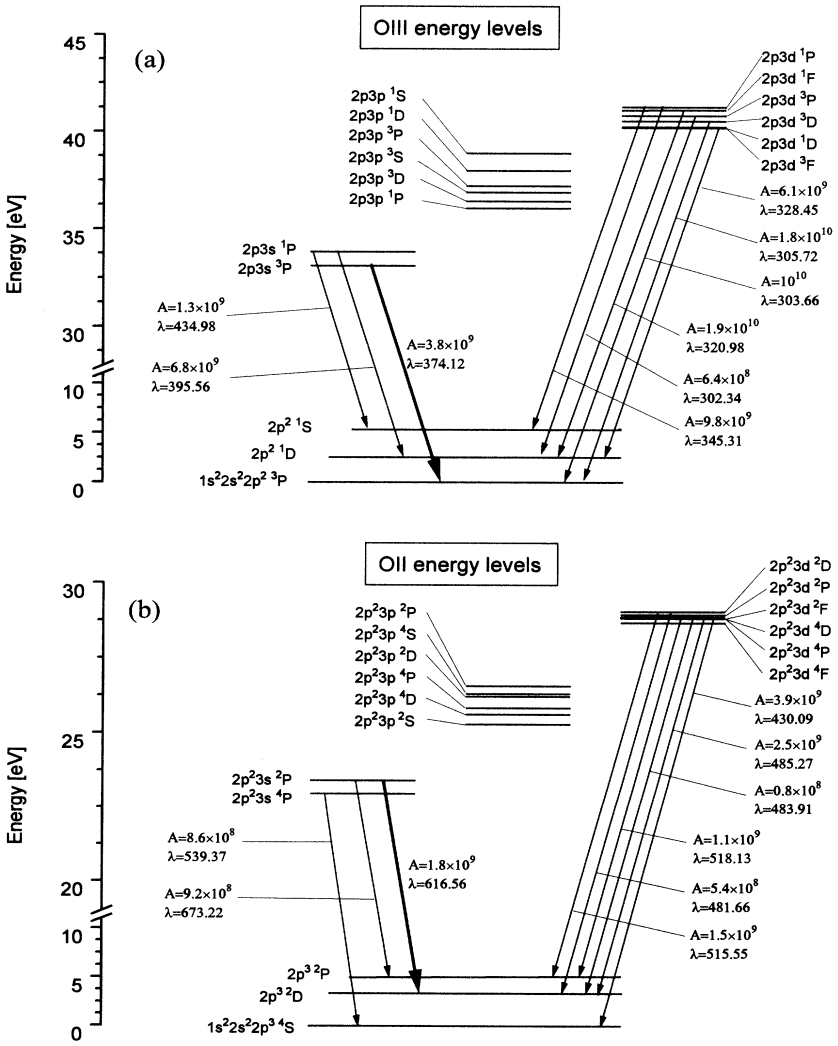

FIG. 6. Energy levels, wavelengths, and radiative decay probabilities for transitions in O III (a) and O II (b) ions.

that for oxygen molecules the ionization potentials are lower than for atoms, therefore, the corresponding electron temperatures will also be lower.

Throughout this paper, we assume a three-body recombination as the dominant pumping mechanism. But it should be noted that in the case of optical field ionization of molecules, additional pumping processes can exist. As was shown in [9], optical field ionization of simple molecules (i.e., diatomic and triatomic) occurs prior to any considerable fragmentation. If the ionization process creates a strong charge asymmetry inside the molecule, then one of the ion fragments can be produced in an excited state due to electron transfer from the lower charged ion (or neutral) to the higher charged ion during the fragmentation. Another possibility is related to the pumping due to the charge transfer processes in collisions of ions with molecules from the surrounding gas. This can be an effective pumping mechanism. The ionic fragments are accelerated during the fragmentation via Coulomb repulsion and their angular distribution is strongly anisotropic with the maximum ion flux along the direction of the laser field. More detailed information on multielectron dissociative ionization of molecules in an intense laser field can be found in [14].

For experiments performed in the confocal geometry (see below) the transverse size of the plasma channel created in a gas jet (cell) is small, $d \sim 10 - 100$ μm. Therefore, part of the fast electrons (especially those that appeared during the last ionization stage, with $T = T_3$), which are moving along the direction of the laser field, can leave the plasma channel region without any interaction within the characteristic time $\sim d/v_{\|}$, where $v_{\|}$ is the corresponding thermal velocity. Colder electrons will remain captured inside the plasma channel due to its positive charge. Therefore, it is reasonable to expect that the effective temperature in the plasma channel will be lower than $T_{\text{eff}} < (T_1 + T_2)/2 \sim 5$ eV, since the hottest electrons from the last ionization stage will be rapidly lost. If T_{eff} will be lower than the energy differences between the $2p3p$, $2p3d$ and $2p3s$, $2p3p$ states in O III [see Fig. 6(a)], $T_{\text{eff}} < 2-3$ eV, then collisional deexcitation of $2p3d$ and $2p3p$ states will provide an efficient population transfer into the $2p3s$ states. Recall that the sufficient pumping rate for the creation of a population inversion between $2p3s(^3P)$ and $2p^2(^3P)$ states is $W_p = A_{21}/10$. The radiative decay probability of the $2p3s(^3P)$ state is 10 times smaller than in the case of the L_α transition in H-like Li ions, where amplification has been observed [3]. Therefore, in comparison with H-like Li ions the necessary conditions for the inversion in O III ions are considerably simplified, since the pumping rate can be 100 times slower.

There is an additional advantage of lasing to the ground electron configuration in complex ions. It is related to the splitting of this configuration (due to electrostatic interaction) on different LS terms. Therefore, the lower laser level (LS term) belonging to the ground electron configuration can be located above the actual ground state of this ion. This is illustrated in Fig. 6(b) for O II ions, where an inversion can be created on the $2p^23s(^2P)$-$2p^3(^2D)$ transition with $g_1/g_2 = 5/3$. The lower laser level is located above the $2p^3(^4S)$ ground state. This creates an exit channel out of the lower laser level due to electron-impact deexcitation and simplifies the threshold conditions for lasing. This depopulation mechanism can be efficient in the case of a sufficiently high plasma density and when the electron temperature is smaller than the corresponding energy difference between the lower laser level and the actual ground state. For O II ions, electron temperatures of the order of $T_{\text{eff}} \sim 1$ eV are necessary.

In the next section experimental investigations of possible soft-x-ray lasing in O II, O III, C III, and N III ions are discussed.

IV. EXPERIMENTAL RESULTS AND DISCUSSIONS

In our experiments, a commercial, high repetition rate (10 Hz), femtosecond Ti:sapphire laser system is used (BMI model Alpha 10A). A detailed description of the principal set-up is given in [15]. This system provides 150-fs laser pulses at 773 nm with a pulse energy of 80 mJ.

The laser radiation is focused with a $f/12$ lens ($f =$ 250 mm) into gas jets, as it is shown in Fig. 7. As gaseous media, O_2, CO_2, and N_2 gases are used. They are injected into the vacuum chamber (10^{-5} Torr) by a pulsed nozzle (General Valve Corporation, model Iota One), which is synchronized with the laser system. The nozzle is opened for about 200 μs. The backing pressure can be varied in the range of 50 – 3000 mbar. The nozzle has three output holes, with a diameter of 300 μm each. The distance between the centers of these holes is 500 μm. These holes can be opened and closed with a mechanical shutter. This provides a possibility for a restricted variation of the plasma length. Soft-x-ray spectra are recorded in the direction of beam propagation by a grazing incidence monochromator (Jobin Ivon, LHT 30, 550 lines/mm gold grating, spectral resolution ~ 0.3 nm) in combination with microchannel plates (Galileo Chevron, 32-mm diameter). All spectra are time integrated by a boxcar averager (EGG, mod. 162). The scanning speed of the monochromator is 10 nm/min.

To determine the laser beam quality, we have performed measurements of the focal spot size with the help

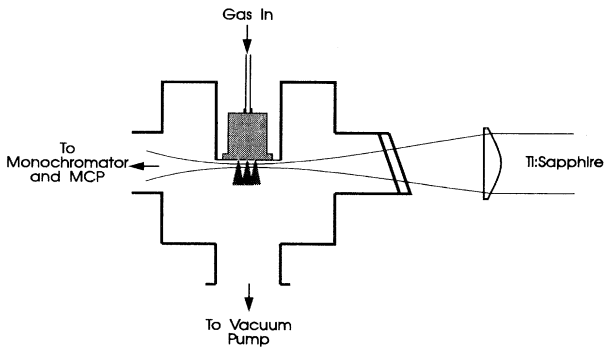

FIG. 7. Experimental setup.

of the knife-edge method [16]. These measurements were performed at atmospheric pressure with a strongly attenuated laser beam. The dimensionless factor $M^2 = 3.5$, characterizing the resemblance of our laser beam to a diffraction-limited Gaussian beam, was measured. When the laser radiation is focused into the gas jet with the $f = 250$-mm lens, the minimum radius of the focused laser beam (beam waist), $w_0 = M^2 f\lambda/\pi w_s$, is 21.5 μm, where $w_s \simeq 1$ cm is the initial beam radius. The Rayleigh length, $z_R = w_0 f/w_s$, is of the order of 540 μm, and the confocal parameter ~ 1.1 mm. The estimated maximum laser intensity in the focal spot is 4×10^{16} W/cm^2. However, the actual intensity in our experiments may well have been 2 – 3 times lower. This intensity is still large enough for the optical field ionization of O III ions over the length of $\simeq 1.5$ mm in the confocal geometry.

In Fig. 8, an example of a plasma spectrum produced in O_2 gas jets is shown for a backing pressure of 160 mbar and 3 holes open. As can be seen, the O III $2p3s\,(^3P)$-$2p^2\,(^3P)$ line at $\lambda_1 = 37.412$ nm is anomalously strong and absolutely dominating in the spectrum. The intensity of the O III $2p3s(^1P)$-$2p^2(^1D)$ line at $\lambda_2 = 39.556$ nm is surprisingly low. The $2p3s$ (^1P) and (^3P) levels are located close to each other [see Fig. 6(a)], and in the case of a Boltzmann distribution between them (and $\Delta E \ll T$) the intensity ratio of lines originating from these levels, defined by the ratio of the corresponding gA values, should be $I_1/I_2 \sim 1.7$. The observed ratio $I_1/I_2 \sim 9$ is very far from this value. This cannot be explained by a strong reabsorption of the low intensity line. Possible explanations are the presence of a stronger pumping mechanism of the triplet state, very low electron temperature ($T < \Delta E$), and/or amplification of the high-intensity line.

Note that in our experiments we are not able to distinguish between the different pumping mechanisms, such as three-body recombination or charge transfer in ion-molecule collisions, when ions leave the plasma (since the electron temperature and plasma density were not directly measured). In principle, both pumping processes can be important. But with the growth of the plasma density the role of three-body recombination pumping increases faster due to its quadratic dependence on electron density. Since we observe that the $2p3s(^3P)$-$2p^2(^3P)$ line remains the strongest in the spectra up to a relatively high backing pressure $\sim$ 800 mbar, we conclude that the three-body recombination pumping is the dominant mechanism.

As can also be seen in Fig. 8, the $2p3d$-$2p^2$ lines are very weak. This can be explained when we assume that the actual electron temperature is lower than the energy differences between the $2p3p$, $2p3d$ and $2p3s$, $2p3p$ levels [see Fig. 5(a) and discussions in Sec. III], $T < 2 - 3$ eV. In this case, collisional deexcitation of $2p3d$ levels (due to $2p3d$-$2p3p$ transitions), which is faster in our experimental conditions than their radiative decay to the ground states, provides an efficient quenching of $2p3d$-$2p^2$ lines. When electrons are hot, $T > 5$ eV, the intensities of these lines will grow due to collisional excitation from $2p3s$ and metastable $2p3p$ states.

The O IV $3s(^2S)$-$2p(^2P)$ line at 27.983 nm is clearly seen in the spectrum. This indicates that the laser intensity was sufficient for the optical field ionization of O III ions. Raman heating and electron-impact collision ionization to the O IV stage can be ruled out. The assumption about high electron temperature contradicts our observations — very low intensities of $3d$-$2p$ lines. Moreover, the laser intensity and the particle density in the gas jet are too low for this mechanism to be effective.

To verify the possibility of amplification on the $2p3s(^3P)$-$2p^2(^3P)$ line, the number of open holes was varied. A nonlinear intensity growth in this line was observed. One sequence of the recorded spectra is shown in Fig. 9. The backing pressure was 165 mbar. The gain

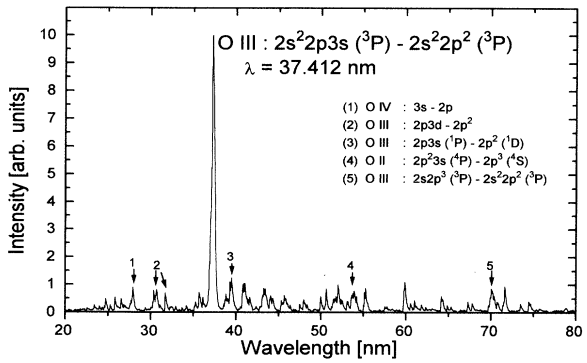

FIG. 8. An example of a "longitudinal" spectrum of a plasma produced in an oxygen gas jet at a backing pressure of 160 mbar.

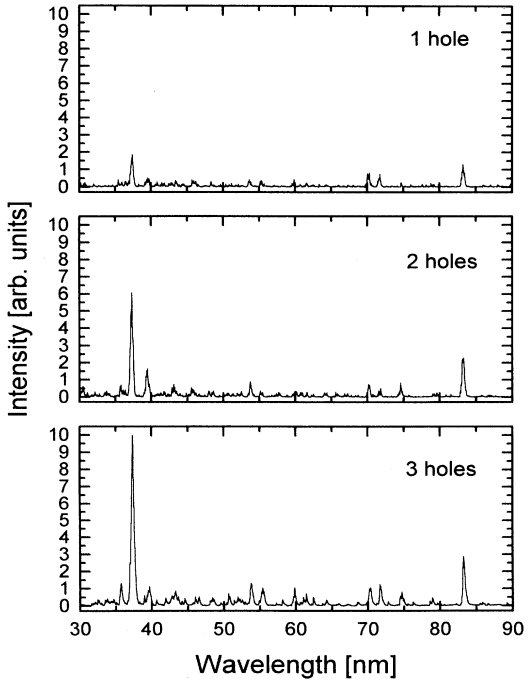

FIG. 9. Oxygen spectra for various numbers of open holes (backing pressure is 165 mbar).

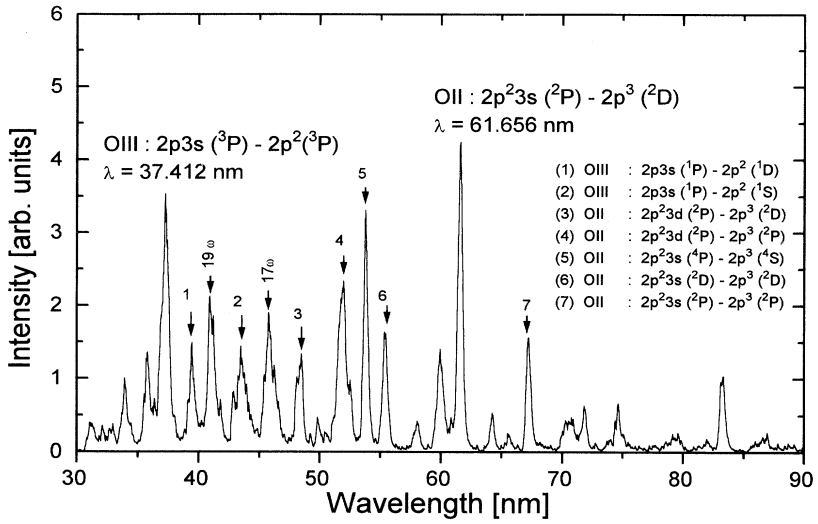

FIG. 10. An example of a spectrum produced at a backing pressure of 900 mbar in oxygen.

coefficient that can be estimated from these (and other) data is > 10 cm^{-1}. This amplification is not a geometrical artifact, since we observe linear growth of intensities for several low opacity nonlasing lines. This also supports our assumption of more or less uniform conditions along the lasing axis. Note that the pressure in a gas jet is at least 10 times lower than the backing pressure. As shown below, at these low densities the refractive defocusing of the laser radiation can be neglected.

The small angle ϕ of the laser beam refraction due to the density gradient (defocusing angle) can be estimated from

$$\phi \simeq \frac{L|\nabla n|}{n} \simeq \frac{L}{d}\left(\frac{\omega_p}{\omega}\right)^2, \tag{11}$$

where $L \sim 1$ mm is the plasma length, $d \sim 45$ μm is the laser beam diameter, $n \simeq 1 - \omega_p^2/2\omega^2$ is the index of refraction due to free electrons, and ω_p is the plasma frequency. We assume here that the electron density gradient length is of the order of the laser beam radius. Refractive defocusing can be neglected if ϕ remains smaller than the half-angle of the laser beam divergence $\theta = w_s/f$. The condition $\phi < \theta$ is equivalent to

$$N_e < \frac{1}{16\pi a_0^3}\left(\frac{dw_s}{Lf}\right)\left(\frac{\hbar\omega}{\mathcal{R}}\right)^2, \tag{12}$$

where N_e is the electron density, $a_0 = 0.529 \times 10^{-8}$ cm is the Bohr radius. For our experimental conditions Eq. (12) gives $N_e < 3 \times 10^{18}$ cm^{-3}. This is definitely fulfilled at the backing pressure of 165 mbar used before.

In Fig. 10 an example of a "normal" spectrum produced at a backing pressure of 900 mbar is shown. In this case, due to a strong defocusing of the short pulse laser radiation, field ionization of O III ions over the whole plasma length is impossible and O II lines become strong. Several harmonics of the pump laser radiation can be seen in this spectrum. Note that the ratio I_1/I_2=2.3 is still bigger than 1.7. If the origin of this difference is due to the Boltzmann exponent, which was not taken into account, the electron temperature should be $T \sim 2$ eV. The indication that even for such densities the plasma remains relatively cold follows again from the relatively low intensities of $2p3d$-$2p^2$ lines.

To test the possibility of lasing on the $2p^23s(^2P)$-$2p^3(^2D)$ transition at 61.656 nm, which was suggested in Sec. III, the backing pressure was reduced to 700 mbar to ensure that O II ions are completely ionized. Examples of our spectra for a different number of open holes are shown in Fig. 11. A nonlinear growth of the corresponding line intensity can be seen. In contrast, the intensities of the other lines remain approximately constant, which can be explained by their reabsorption at this high pres-

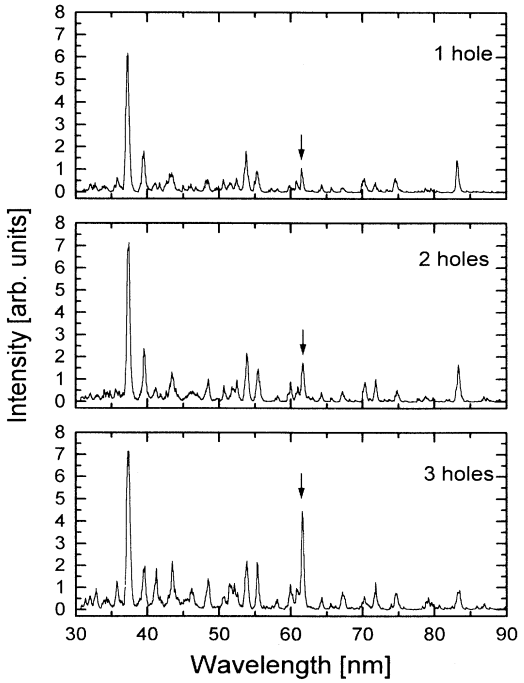

FIG. 11. Oxygen spectra for various numbers of open holes (backing pressure is 700 mbar).

sure. An estimate of the corresponding gain coefficient (with the Linford formula [17]) gives a very high gain value of ~ 25 cm^{-1}. Note that the defocusing of laser radiation, which cannot be neglected in this case, leads to some uncertainty in the gain value.

The evidence for amplification demonstrated above (Fig. 9 and Fig. 11) is not overwhelming. The time-resolved soft-x-ray spectroscopy technique could provide more detailed information on the transient lasing. As discussed in [4], modification of the axial plasma expansion with the plasma length might simulate gain conditions. This is ruled out in our case since we use separate gas jets.

We have repeated our experiments with the CO_2 and N_2 gases instead of O_2. In Figs. 12(a) and 12(b) energy levels for C III ions and a spectrum recorded at 150-mbar backing pressure are shown. We expected to observe amplification on the C III $2s3s(^3S)$-$2s2p(^3P)$ line ($g_1/g_2 = 3$) at 53.823 nm. As can be seen, this line is indeed very strong. Unfortunately, in the time-integrated spectra we have only observed an approximately linear dependence on plasma length for this and also for the

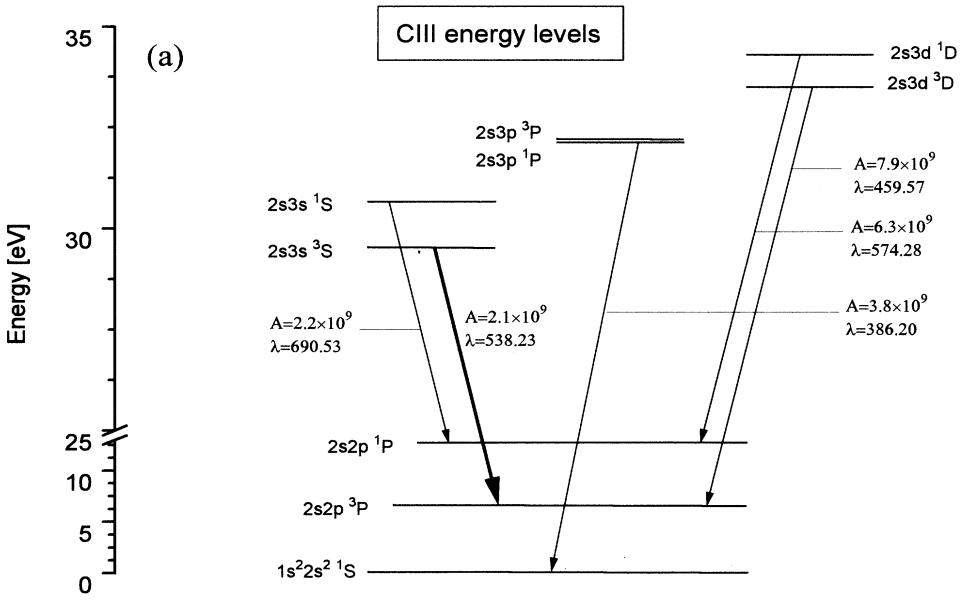

FIG. 12. Energy levels for C III ions (a) and a spectrum of a plasma (b) produced in a CO_2 gas jet at a backing pressure of 150 mbar.

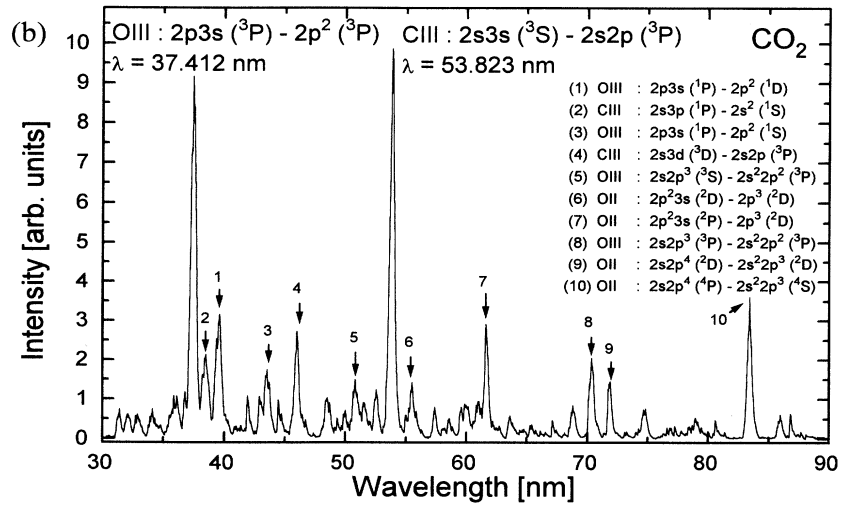

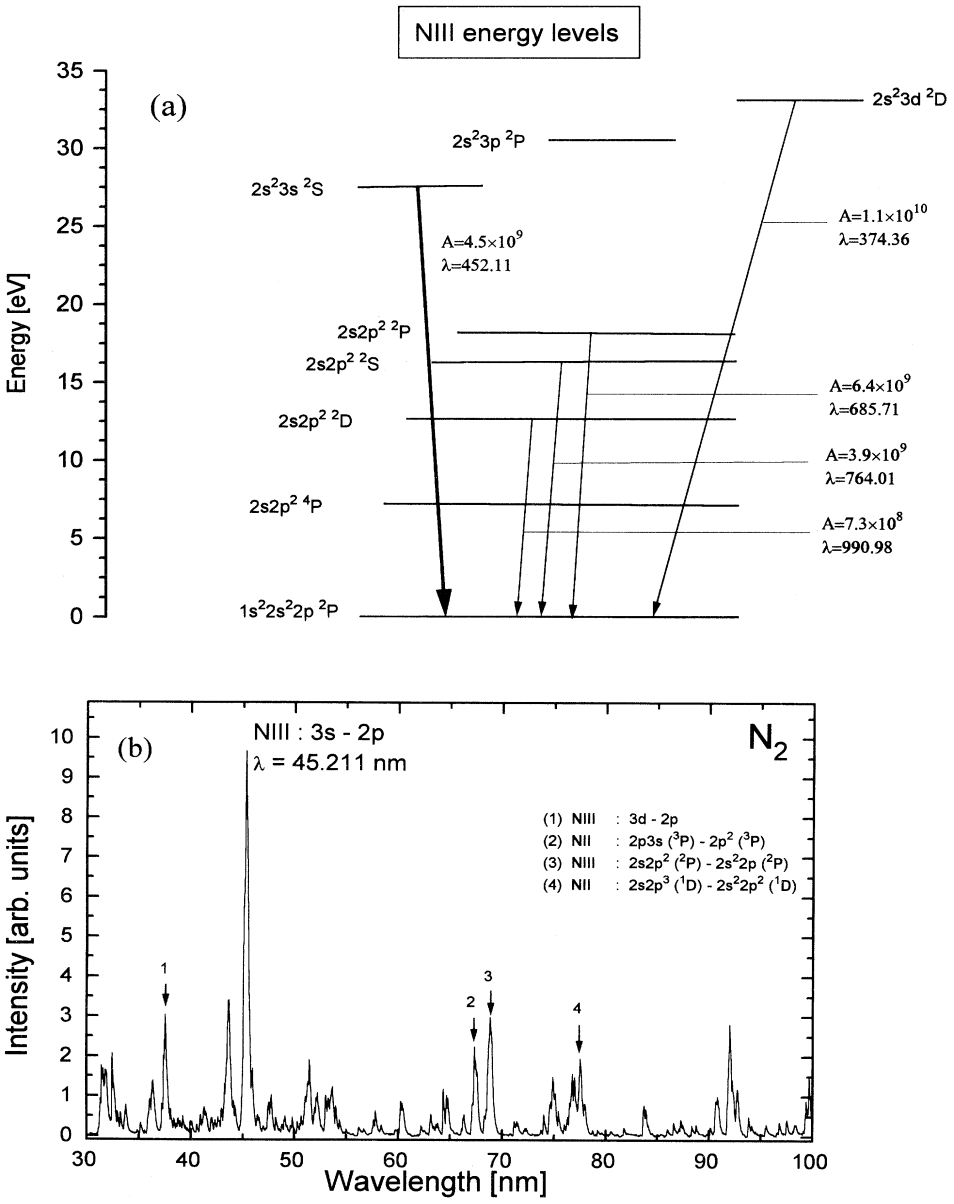

FIG. 13. Energy levels for N III ions (a) and a spectrum of a plasma (b) produced in a N_2 gas jet at a backing pressure of 150 mbar.

O III line at 37.412 nm.

In Figs. 13(a) and 13(b) energy levels for N III and a spectrum recorded at a backing pressure of 150 mbar are shown. As was expected, the $3s$-$2p$ line at 45.211 nm is again the strongest in the spectrum. But no amplification was observed. These results are preliminary, more sophisticated experimental and theoretical investigations are necessary. It is planned to repeat the experiments with an increased pump laser energy and an improved nozzle design.

V. CONCLUSION

We have suggested that favorable conditions for soft-x-ray lasing to the ion ground states can be created in complex ions. Low charged Be-, B-, C-, and N-like ions were studied as potential candidates. Amplification on the $2p3s(^3P)$-$2p^2(^3P)$ transition, (λ = 374.12 Å), in O III ions and on the $2p^23s(^2P)$-$2p^3(^2D)$ transition, (λ = 616.56 Å), in O II ions has been observed.

[1] N.H. Burnett and P.B. Corkum, J. Opt. Soc. Am. B **6**, 1195 (1989); N.H. Burnett and G.D. Enright, IEEE J. Quantum Electron. **26**, 1797 (1990); B.M. Penetrante and J.N. Bardsley, Phys. Rev. A **43**, 3100 (1991); B.E. Lemoff, C.P.J. Barty, and S.E. Harris, Opt. Lett. **19**, 569 (1994).

[2] P. Amendt, D.C. Eder, and S.C. Wilks, Phys. Rev. Lett. **66**, 2589 (1991); D.C. Eder, P. Amendt, and S.C. Wilks,

Phys. Rev. A **45**, 6761 (1992); P. Amendt, D.C. Eder, R.A. London, and M.D. Rosen, *ibid.* **47**, 1572 (1993).

[3] Y. Nagata, K. Midorikawa, S. Kubodera, M. Obara, H. Tashiro, and K. Toyoda, Phys. Rev. Lett. **71**, 3774 (1993); D.C. Eder, P. Amendt, L.B. DaSilva, R.A. London, B.J. MacGowan, D.L. Matthews, B.M. Penetrante, M.D. Rosen, S.C. Wilks, T.D. Donnelly, R.W. Falcone, and G.L. Strobel, Phys. Plasmas **1**, 1744 (1994); T.D. Donnelly, T.E. Glover, E.A. Lipman, M. Hofer, R.W. Falcone, L. DaSilva, S. Morwka, and D.C. Eder, in *High Field Interactions and Short Wavelength Generation*, OSA Technical Digest Series Vol. 16 (OSA, St. Malo, France, 1994), p. 157.

[4] T. Ozaki and H. Kuroda, Phys. Rev. E **51**, R24 (1995).

[5] B.E. Lemoff, G.Y. Yin, C.L. Gordon III, C.P.J. Barty, and S.E. Harris, Phys. Rev. Lett. **74**, 1574 (1995).

[6] A.E. Siegman, *Lasers* (University Science Book, Mill Valley, CA, 1986).

[7] S. Augst, D. Strickland, D.D. Meyerhofer, S.L. Chin, and J.H. Eberly, Phys. Rev. Lett. **63**, 2212 (1989).

[8] L.V. Keldysh, Zh. Eksp. Teor. Fiz. **47**, 1945 (1964) [Sov. Phys. JETP **20**, 1307 (1965)].

[9] S.L. Chin, Y. Liang, J.E. Decker, F.A. Ilkov, and M.V. Ammosov, J. Phys. B **25**, L249 (1992); T.D.G. Walsh, J.E. Decker, and S.L. Chin, *ibid.* **26**, L85 (1993); P. Dietrich, D.T. Strickland, and P. Corkum, *ibid.* **26**, 2323 (1993).

[10] P. Corkum, N. Burnett, and F. Brunel, Phys. Rev. Lett. **62**, 1259 (1989).

[11] A. Nikishov and V. Ritus, Zh. Eksp. Teor. Fiz. **50**, 255 (1966) [Sov. Phys. JETP **23**, 168 (1966)]; A.M. Perelomov, V.S. Popov, and M.V. Terent'ev, *ibid.* **50**, 1393 (1966) [**23**, 924 (1966)]; N.B. Delone and V.P. Krainov, J. Opt. Soc. Am. B **8**, 1207 (1991).

[12] B.N. Chichkov (unpublished).

[13] W.P. Leemans, C.E. Clayton, W.B. Mori, K.A. Marsh, A. Dyson, and C. Joshi, Phys. Rev. Lett. **68**, 321 (1992); W.P. Leemans, C.E. Clayton, W.B. Mori, K.A. Marsh, P.K. Kaw, A. Dyson, C. Joshi, and J.M. Wallace, Phys. Rev A **46**, 1091 (1992).

[14] K. Codling and L.J. Frasinski, J. Phys. B **26**, 783 (1993); C. Cornaggia, M. Schmidt, and D. Normand, *ibid.* **27**, L123 (1994); L.J. Frasinski, P.A. Hatherly, K. Codling, M. Larson, A. Persson, and C.G. Wahlström, *ibid.* **27**, L109 (1994); P. Dietrich, D.T. Strickland, M. Laberge, and P.B. Corkum, Phys. Rev. A **47**, 2305 (1993); T.S. Luk, D.A. Tate, K. Boyer, and C.K. Rhodes, *ibid.* **48**, 1359 (1993).

[15] J.D. Kmetec, J.J. Macklin, and J.F. Young, Opt. Lett. **16**, 1001 (1991).

[16] R.D. Jones and T.R. Scott, Laser Focus World **29**, 123 (1993).

[17] G.J. Linford, E.R. Peressini, W.R. Sooy, and M.L. Speath, Appl. Opt. **13**, 379 (1974).